

Paper

The Growth Mechanism of Al-doped ZnO using Oxygen Controlled Seed Layer in Si based Thin Film Solar Cells

Minho Joo*, Huiyoun Shin, Jangho Lee, Seungkyu Moon, Taeho Moon, and Kyuho Park
Devices and Materials Laboratory, LG Electronics Advanced Research Institute, Seoul 137-724, Korea
*minho.joo@lge.com

(Received : October 9, 2010; Accepted : December 14, 2010)

We studied the growth mechanism of Al-doped ZnO (AZO) films using seed layers for enhancing the performance of transparent conducting oxides (TCOs) in the thin film solar cells. We carried out two-step processes for the deposition of AZO films. Seed layers were deposited on glass substrate as a function of Ar/O₂ gas flow ratio. We show the results of our investigation on the micro-structural properties of AZO seed layers using transmission electron microscopy (TEM). The elemental composition and electronic structure changes with the deposition conditions were examined using energy dispersive X-ray (EDX) and reflective electron energy loss spectroscopy (REELS). The optical and electrical characteristics of AZO film using the seed layer with Ar/O₂ = 9/1 show a high haze value of 88% at 500 nm and a resistivity value of $3.7 \times 10^{-4} \Omega\text{-cm}$.

1. Introduction

Transparent conducting oxides (TCOs) have many applications such as electro-optical devices, flat panel displays, and thin film solar cells [1, 2]. TCOs consist of degenerate wide band gap with low resistance and high transparency in the visible region. ZnO is a very attractive oxide semiconductor which possesses wide and direct band gap (3.3 eV), large excitonic binding energy (60 meV), and high transparency in the visible range. Doping ZnO with high-valence elements such as Al, Ga and In dramatically increases its conductivity. In the solar cell applications, TCOs make an important role of electrodes and passage into light absorption layers. Surface texturing of TCOs extends the effective path length of the scattered light within absorption layers, which results in the minimization of the thickness of the absorption layers for decreasing production costs [1]. Al-doped ZnO (AZO) has a promising material for Si based thin film solar cells. AZO is easily textured by wet-chemical etching and has large feature size compared to SnO₂:F. And, the large feature size of the surface texture results in a high haze (diffused light/total-transmitted light), which increases the degree of light trapping [2].

There have been a few reports on the use of seed layers such as ZnS, Lu₂O₃, and SiC for improving the crystallinity of ZnO films, but these seed layers incur an additional process cost [4-6].

Recently, Kang *et. al.* reported two-step process involving the control of the oxygen flow, and a drastic improvement of crystallinity using a seed layer [3]. However, the growth mechanism of AZO using a seed layer is not completely understood. In this paper, we report the growth mechanism of AZO films using seed layers for enhancing the crystallinity of TCOs in the thin film solar cells.

2. Experimental Configurations

The AZO films were deposited on Corning 1737 glass by the use of pulsed-DC magnetron sputtering using a ZnO:Al target having 2 wt.% Al₂O₃ at a deposition temperature of 320 °C. In order to examine the characteristics of the ZnO:Al films as a function of the deposition conditions of the seed layer, seed layers were prepared with various argon to oxygen pressure ratios (Ar/O₂) ranging from 24/1 to 4/1. The bulk layers were deposited under pure Ar after the deposition of seed layers. Also, a sample without a seed layer was prepared as a reference. The working pressure was fixed at 1.5 mTorr during all of the deposition steps. Surface texturing was performed by means of wet-chemical etching using dilute HCl acid (0.5%) at room temperature in order to investigate the light-scattering characteristics.

The local strains of seed layers were characterized by X-ray diffraction (XRD; Rigaku

D/MAX-IIIC). The surface morphology was examined over a scan area of $10 \times 10 \mu\text{m}^2$ by atomic force microscopy (AFM; Digital Instrument Nanoscope IIIa). The change of growth mode with different seed-layer conditions was systematically examined by transmission electron microscopy (TEM; Philips CM20 T/STEM). For the investigation of surface properties of seed layers, we conducted reflected electron energy loss spectroscopy (REELS) using low electron energy (200 eV) by cylindrical mirror analyzer (CMA). The transmittance was obtained in the range from 350 to 1100 nm by means of a spectrophotometer (Varian Cary 5000) and the haze values were calculated with specular components and diffuse components. The four-point probe method was also used to evaluate the sheet resistance and resistivity.

3. Results

Fig.1 shows qualitative estimation of seed layers as a function of Ar to O₂ ratios. X-ray diffraction peak widths Δk (full width at half maximum) were fitted with two peaks of (002) and (004), using a Lorentzian function, as shown in the inset of Fig. 1. The strain can be deduced from the slope of the Δk vs k graph. It is known the simple expression,

$$\Delta k = 2\pi/D + (\Delta d/d)/k;$$

where D the effective grain size suggested by Scherrer, and $\Delta d/d$ is the local strain derived from the Bragg relation (d is the lattice constant and Δd is the nonuniform distribution of the lattice constant) [7-9]. Local strain is possibly due to point defects, off-stoichiometry, stacking faults, dislocations, etc. As the oxygen pressure increases, a decrease in the local strain (increase of crystallinity) is clearly shown (Fig. 1). Furthermore, it is shown that the increase of crystallinity is saturated at higher oxygen pressures for Ar/O₂ < 9/1. The resistivities, calculated from the sheet resistance and bulk-layer thickness, were $4.7 \times 10^{-4} \Omega \cdot \text{cm}$ (no seed), $4.1 \times 10^{-4} \Omega \cdot \text{cm}$ (Ar/O₂ = 24/1), $4.0 \times 10^{-4} \Omega \cdot \text{cm}$ (Ar/O₂ = 18/1), and $3.7 \times 10^{-4} \Omega \cdot \text{cm}$ (Ar/O₂ = 9/1). The decrease of resistivity with increasing oxygen pressure correlated well with the change of crystallinity, as shown in Fig. 1. It should be noted here that the seed layers deposited in the presence of oxygen flow were highly resistive. For example, the sheet resistance of the seed layer deposited under the conditions of Ar/O₂ = 9/1 was $\sim 100 \text{ k}\Omega/\square$.

The surface morphology of seed layers

according to Ar to O₂ ratios is shown in Fig. 2. As-grown seed layers of AZO films had different morphology values in Fig. 2a and b. In Fig. 2c and 2d, AZO films, which were deposited on the seed layers with the thickness of 100 nm of Fig. 2a and 2b, showed same morphological trends like the seed layers of Fig. 2a and 2b. The RMS value of the surface roughness increases with decreasing Ar to O₂ ratios.

The crystalline structures and elemental analysis of seed layers were performed with TEM/STEM. The cross-sectional samples of seed layers were prepared by focused ion beam (FIB). The thickness of seed layers was fixed to 80 nm, and the samples were sequentially prepared with an increase in bulk thickness of 100 nm in order to observe the growth mode. The AZO films with

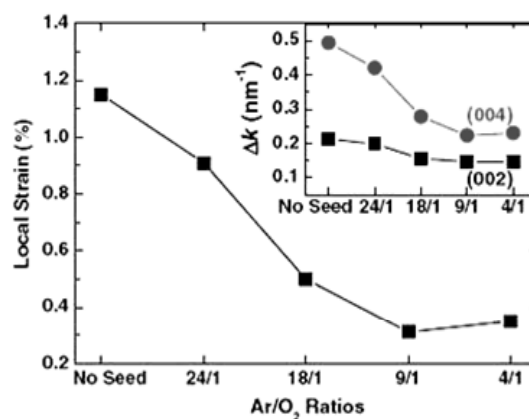


Fig. 1. Local strains ($\Delta d/d$) of the AZO films with different Ar to O₂ flow ratios during the deposition of seed layers. The inset shows the variation in the XRD peak widths, Δk (full width at half maximum), of the (002) and (004) diffractions.

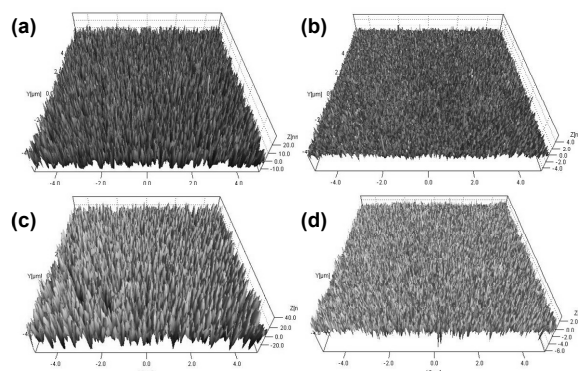


Fig. 2. AFM images of AZO film for seed layers with different Ar to O₂ pressure ratios corresponding to (a) Ar/O₂ = 24/1, (b) Ar/O₂ = 9/1. Films of (c) and (d) were deposited with the thickness of 100 nm on the seed layers of (a) and (b) respectively. The RMS values of the surface roughness; (a) 6.94 nm, (b) 0.69 nm, (c) 14.7 nm, and (d) 0.96 nm.

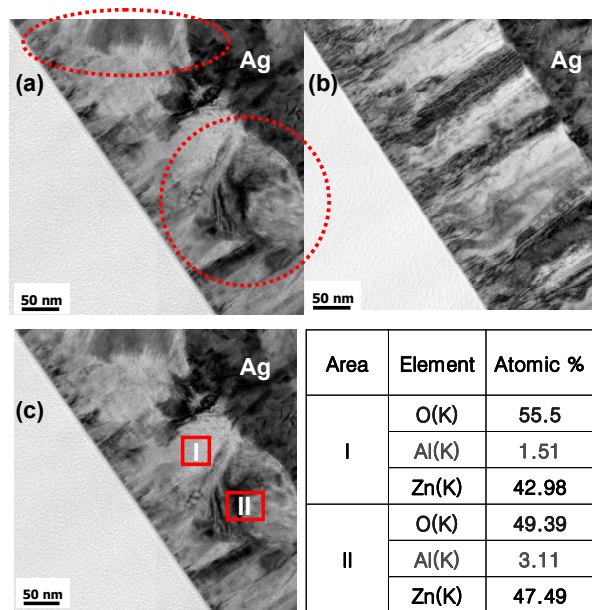


Fig. 3. Cross-sectional TEM images of AZO films with different Ar to O₂ ratios; (a) Ar/O₂ = 24/1, (b) Ar/O₂ = 9/1. Composition analysis was performed with EDX of STEM mode in (c) Ar/O₂ = 24/1. Ag layer was deposited on the AZO films for preventing the surface damage of AZO film during the sample preparation of TEM using FIB.

different seed layers show clearly different microstructures. The seed layer under the condition of Ar/O₂ = 24/1 shows grains that result in the formation of a hillock over some distance. The shape of the grains is maintained throughout the bulk thickness of 100 nm. In that Ar/O₂ = 24/1 condition of seed layer, two types of growth were observed with columnar and hillock structures. However, the seed layer of Ar/O₂ = 9/1 condition shows vertical growth and flat surface. Elemental analysis of AZO films was performed to investigate the composition differences of columnar structure and hillock grain with EDX in STEM mode. Fig. 3c shows elemental analysis areas of the AZO films with the condition of Ar/O₂ = 24/1 in Fig. 3a. Area II has more metallic elements than Area I. It is noted that the grain of hillock has more surface defects by metal rich layer during growing.

REELS characterization was conducted to observe the surface band gap for the differences of surface states with the growth conditions of seed layers in Fig. 4. As the increase of Ar/O₂ ratios, the surface band gap values decrease gradually. The band gap decrease with the increase of Ar/O₂ ratios may be occurred by the hillock surface and the metal rich surface in Fig. 3a and 3c. Metal rich

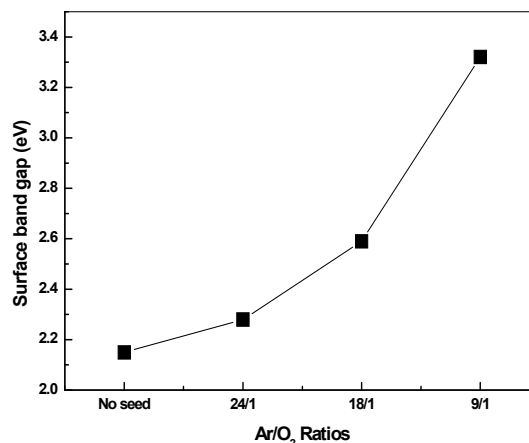


Fig. 4. Surface band gap of seed layers with different Ar/O₂ ratios was characterized by REELS method using electron energy, E_p = 200 eV.

surface and high RMS valued morphology can be understood that they make an important role of increasing surface defects on seed layers.

Fig. 5 shows the total transmittance and haze values of the etched AZO films after grown on the seed layers with different Ar/O₂ ratios. The RMS values of the surface roughness for the etched AZO films gradually increase to 72, 83, 100, and 142 nm, respectively, with increasing oxygen pressure. The haze values increase with increasing oxygen pressure. Especially interesting is the fact that the sample deposited under Ar/O₂ ratio = 9/1 shows a very high haze value of 88 % at 500 nm.

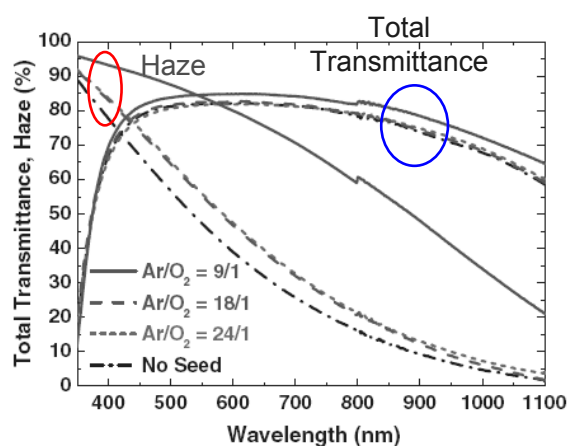


Fig. 5. Total transmittance and haze values (diffused/total transmitted) of the AZO films with different Ar to O₂ ratios during the deposition of the seed layers.

This result may be explained by the large columnar structure as shown in Fig. 3b. Further studies concerning with texturing morphology and solar cell performance are under way.

4. Conclusion

In summary, AZO films were deposited by DC-pulsed magnetron sputtering using two-step process. The seed layers were prepared with various Ar/O₂ ratios, and the bulk layers were deposited under pure Ar. The growth mode was systematically investigated with surface and structure analysis. The sample under the condition of Ar/O₂ = 24/1 showed an abnormal grain growth and high metallic surface. In contrast, the sample grown under the condition of Ar/O₂ = 9/1 showed large lateral growth and wide surface band gap. Also, surface state controlled by Ar/O₂ ratio had an important role of the growth of AZO film on the seed layer. In the condition of Ar/O₂ ratio = 9/1, AZO thin film had a high haze value of 88% at 500 nm and a resistivity value of $3.7 \times 10^{-4} \Omega \cdot \text{cm}$. Detailed studies of the correlation between AZO film and solar cell performance will be needed in near future.

5. References

- [1] J. Muller, B. Rech, J. Springer and M. Vanecek, *Solar Energy* **77**, 917 (2004).
- [2] Y. Zhao, S. Miyajima, Y. Ide, A. Yamada and M. Konagai, *Jpn. J. Appl. Phys.* **41**, 6417 (2002).
- [3] D.-W. Kang, S.-H. Kuk, K.-S. Ji, S.-W. Ahn, and M.-K. Han, *Mater. Res. Soc. Symp. Proc.* **A07-19**, 1153 (2009).
- [4] T. Onuma, S. F. Chichibu, A. Uedono, Y.-Z. Yoo, T. Chikyow, T. Soda, M. Kawasaki, and H. Koinuma, *Appl. Phys. Lett.* **85**, 5586 (2004).
- [5] W. Guo, A. Allenic, Y. B. Chen, X. Q. Pan, W. Tian, C. Adamo, and D. G. Schlom, *Appl. Phys. Lett.* **92**, 072101 (2008).
- [6] Y. Zhang, H. Zheng, J. Su, B. Lin, and Z. Fu: *J. Lumin.* **124**, 252 (2007).
- [7] P. Scherrer, *Göttinger Nachrichten* **2**, 98 (1918).
- [8] B. E. Warren: *X-ray Diffraction*, p. 257, Dover, New York (1990).
- [9] T. Kim, J. Oh, B. Park, and K. S. Hong, *Appl. Phys. Lett.* **76**, 3043 (2000).